Reactivity of $[SeFe_3(CO)_9]^{2-}$ with Electrophiles: Formation of $[SeFe_2Ru_3(CO)_{14}]^{2-}$, $[SeFe_3(CO)_9(\mu\text{-HgI})]^-$, $Fe_2(CO)_6(\mu\text{-SeCHPhSe})$, and $Se_2Fe_2(CO)_6(\mu\text{-CH}_2)_2$

Minghuey Shieh,* Yi-Chou Tsai, Jiann-Jang Cherng, Mei-Huey Shieh, Horng-Sun Chen, and Chuen-Her Ueng

Department of Chemistry, National Taiwan Normal University, Taipei 11718, Taiwan, Republic of China

Shie-Ming Peng and Gene-Hsiang Lee

Department of Chemistry, National Taiwan University, Taipei 10764, Taiwan, Republic of China

Received September 5, 1996[⊗]

The reactions of the tetrahedral cluster $[SeFe_3(CO)_9]^{2-}$ with some transition-metal complexes and organic halides were investigated. The mixed-metal cluster $[Et_4N]_2[SeFe_2Ru_3(CO)_{14}]$ (**1**) was obtained from the reaction of $[Et_4N]_2[SeFe_3(CO)_9]$ with $Ru_3(CO)_{12}$ in acetone. Further reaction of $[Et_4N]_2[SeFe_3(CO)_9]$ with HgI_2 produces the HgI-bridged cluster $[Et_4N][SeFe_3(CO)_9(\mu\text{-HgI})]$ (**2**). While $[SeFe_3(CO)_9]^{2-}$ reacts with $CHPhCl_2$ to produce the CHPh-bridged cluster $Fe_2(CO)_6(\mu\text{-SeCHPhSe})$ (**3**), treatment with CH_2I_2 forms the major product $Se_2Fe_2(CO)_6(\mu\text{-CH}_2)_2$ (**4**). Complex **1** displays an octahedral metal core with a μ_4-Se atom and two carbonyl groups bridging the Ru−Ru and Ru−Fe bonds. Cluster **2** consists of a $SeFe_3$ core with a HgI fragment bridging one Fe−Fe bond, and cluster **3** exhibits a Se_2Fe_2 butterfly geometry with the wingtip linked by a CHPh moiety. On the other hand, cluster **4** contains a planar Se_2Fe_2 moiety with two CH_2 groups bridging the two Se−Fe bonds. Complexes **1**−**4** have been fully structurally characterized by spectroscopic methods and X-ray diffraction analyses. This paper describes the formation of four different types of clusters from the reactions of $[SeFe_3(CO)_9]^{2-}$ with electrophiles and discusses the role of $[SeFe_3(CO)_9]^{2-}$ and the incoming electrophiles.

Introduction

Selenium-containing transition-metal carbonyl clusters have attracted great attention due to their interesting bonding modes and versatile structural features.[1] Recently, a number of anionic selenium−iron carbonyl clusters have been structurally characterized. Examples include $[SeFe_3(CO)_9]^{2-}$,[2] $[Se_6Fe_6(CO)_{12}]^{2-}$,[3] $[Se_2Fe_5(CO)_{14}]^{2-}$,[3a] $[Fe(CO)_2(Se_4)_2]^{2-}$,[4] $[\{Fe_2Se(CO)_6\}_2(Se_2)]^{2-}$,[5] and $[Fe_2(CO)_6(PSe_5)_2]^{2-}$.[6] Among these anionic clusters, $[SeFe_3(CO)_9]^{2-}$ exhibits a *closo*-tetrahedral geometry with an apical μ_3-Se atom bonded to a triangular Fe_3 plane. It has been demonstrated that $[SeFe_3(CO)_9]^{2-}$ reacts readily with the transition-metal salts $M(OAc)_2$ (M = Hg, Cd) to form the μ_4-M bridging clusters $[\{SeFe_3(CO)_9\}_2M]^{2-}$,[2a] and the basic sites of this cluster may be located around the Fe−Fe bonds. To further understand the affinity of $[SeFe_3(CO)_9]^{2-}$ and other electrophiles, we investigated the reactions of $[SeFe_3(CO)_9]^{2-}$ with other transition-metal complexes and organic geminal halides. Our results show that the tetrahedral cluster anion $[SeFe_3(CO)_9]^{2-}$ either can bond to the electrophiles by sharing one of the Fe−Fe bonds, retaining its parent structure, or can form reactive species with metal fragments by loss of Fe vertices, resulting in some different types of clusters. In this paper, we will present the four new complexes **1**−**4** and discuss the formation of these compounds in terms of the roles of the electrophiles and $[SeFe_3(CO)_9]^{2-}$. During the preparation of this paper, we have learned that complex **4** has also been prepared by another method.[7]

Experimental Section

All reactions were performed under an atmosphere of pure nitrogen using standard Schlenk techniques. Solvents were purified, dried, and distilled under nitrogen prior to use. The compound $[Et_4N]_2[SeFe_3(CO)_9]$ is prepared according to the published method.[2a] Infrared spectra were recorded on a Jasco 5300 IR spectrometer as solutions in CaF_2 cells. ESI mass spectra were obtained on a Fision (VG platform) mass spectrometer. ^1H NMR spectra were recorded with a JEOL 400 (400 MHz) instrument. Elemental analyses were performed on a Perkin-Elmer 2400 analyzer at the NSC Regional Instrumental Center at National Taiwan University, Taipei, Taiwan.

* To whom all correspondence should be addressed.

[⊗] Abstract published in *Advance ACS Abstracts,* January 1, 1997.

(1) (a) Linford, L.; Raubenheimer, H. G. *Adv. Organomet. Chem.* **1991**, *32*, 1. (b) Roof, L. C.; Kolis, J. W. *Chem. Rev.* **1993**, *93*, 1037. (c) Adams, R. D. *Polyhedron* **1985**, *4*, 2003. (d) Bogan, L. E.; Rauchfuss, T. B.; Rheingold, A. L. *J. Am. Chem. Soc.* **1985**, *107*, 3843. (e) Mathur, P.; Mavunkal, I. J.; Rugmini, V.; Mahon, M. F. *Inorg. Chem.* **1990**, *29*, 4838.

(2) (a) Shieh, M.; Tsai, Y.-C. *Inorg. Chem.* **1994**, *33*, 2303. (b) Bachman, R. E.; Whitmire, K. H. *Inorg. Chem.* **1994**, *33*, 2527.

(3) (a) Holliday, R. L.; Roof, L. C.; Hargus, B.; Smith, D. M.; Wood, P. T.; Pennington, W. T.; Kolis, J. W. *Inorg. Chem.* **1995**, *34*, 4392. (b) Shieh, M.; Shieh, M.-H.; Tsai, Y.-C.; Ueng, C.-H. *Inorg. Chem.* **1995**, *34*, 5088.

(4) Rauchfuss, T. B.; Dev, S.; Wilson, S. R. *Inorg. Chem.* **1992**, *31*, 154.

(5) Huang, S.-P.; Kanatzidis, M. G. *Inorg. Chem.* **1993**, *32*, 821.

(6) Zhao, J.; Pennington, W. T.; Kolis, J. W. *J. Chem. Soc., Chem. Commun.* **1992**, 265.

(7) Mathur, P.; Manimaran, B.; Trivedi, R.; Hossain, M. M.; Arabatti, M. *J. Organomet. Chem.* **1996**, *515*, 155.

S0276-7333(96)00767-4 CCC: $14.00

Table 1. Crystallographic Data for $[Et_4N]_2[SeFe_2Ru_3(CO)_{14}]$ (1), $[Et_4N][SeFe_3(CO)_9(\mu\text{-HgI})]$ (2), and $Fe_2(CO)_6(\mu\text{-SeCHPhSe})$ (3)

	1	2	3
formula	$C_{30}H_{40}Fe_2N_2O_{14}Ru_3Se$	$C_{17}H_{20}IFe_3HgNO_9Se$	$C_{13}H_6Fe_2O_6Se_2$
fw	1146.52	956.34	527.80
cryst syst	monoclinic	monoclinic	monoclinic
space group	$P2_1/c$	$P2_1/c$	$P2_1/n$
a, Å	16.917(3)	18.364(3)	8.351(1)
b, Å	11.427(2)	16.708(7)	21.785(4)
c, Å	21.967(6)	19.734(3)	8.953(1)
β, deg	107.02(3)	113.59(1)	95.54(1)
V, Å^3	4060.5(1)	5549(3)	1621.3(5)
Z	4	8	4
D(calcd), Mg m^{-3}	1.984	2.290	2.162
abs coeff, cm^{-1}	27.160	94.969	62.599
diffractometer	Nonius (CAD-4)	Nonius (CAD-4)	Nonius (CAD-4)
radiation, λ(Mo Kα), Å	0.7107	0.7107	0.7107
temp, °C	25	25	25
T_{min}/T_{max}	0.93/1.00	0.79/1.00	0.71/1.00
residuals:[a] R, R_w	0.044; 0.041	0.039; 0.036	0.029; 0.028

[a] The functions minimized during least-squares cycles were $R = \sum|F_o - F_c|/\sum F_o$ and $R_w = [\sum w(F_o - F_c)^2/\sum w(F_o)^2]^{1/2}$.

Reaction of $[Et_4N]_2[SeFe_3(CO)_9]$ with $Ru_3(CO)_{12}$. To a mixture of 0.40 g (0.53 mmol) of $[Et_4N]_2[SeFe_3(CO)_9]$ and 0.34 g (0.53 mmol) of $Ru_3(CO)_{12}$ was added 30 mL of Me_2CO. The mixed solution was heated to reflux overnight, the resultant solution was filtered, and the solvent was removed under vacuum. The oil residue was recrystallized with hexanes/CH_2Cl_2, and the precipitate was then extracted with MeOH to give 0.32 g (0.28 mmol) of the pure compound $[Et_4N]_2[SeFe_2Ru_3(CO)_{14}]$ (**1**; 53% based on $Ru_3(CO)_{12}$). IR (ν_{CO}, CH_2Cl_2): 2029 w, 1969 vs, br, 1749 w, br cm^{-1}. Crystals suitable for X-ray diffraction were grown from a CH_2Cl_2 solution. Anal. Calcd for $[Et_4N]_2[SeFe_2Ru_3(CO)_{14}]$ (**1**): C, 31.43; H, 3.52; N, 2.44. Found: C, 30.98; H, 3.32; N, 2.36.

Reaction of $[Et_4N]_2[SeFe_3(CO)_9]$ with HgI_2. To a mixture of 0.50 g (0.66 mmol) of $[Et_4N]_2[SeFe_3(CO)_9]$ and 0.60 g (1.32 mmol) of HgI_2 was added 30 mL of Me_2CO. The mixed solution was stirred overnight, the resultant solution was filtered, and the solvent was removed under vacuum. The residue was washed with hexanes and then extracted with ether. The ether extract was recrystallized with hexanes/CH_2Cl_2 to give 0.45 g (0.47 mmol) of the pure compound $[Et_4N][SeFe_3(CO)_9HgI]$ (**2**; 71% based on $[Et_4N]_2[SeFe_3(CO)_9]$). IR (ν_{CO}, CH_2Cl_2): 2044 m, 2004 vs, 1984 s, 1963 m cm^{-1}. Crystals suitable for X-ray diffraction were grown from hexanes/CH_2Cl_2 solution. Anal. Calcd for $[Et_4N][SeFe_3(CO)_9HgI]$ (**2**): C, 21.35; H, 2.11; N, 1.46. Found: C, 21.22; H, 1.92; N, 1.35.

Reaction of $[Et_4N]_2[SeFe_3(CO)_9]$ with $PhCHCl_2$. To a solution of 0.51 g (0.67 mmol) of $[Et_4N]_2[SeFe_3(CO)_9]$ in 35 mL of MeCN in an ice/water bath was added 0.20 mL (1.56 mmol) of $PhCHCl_2$. The resulting solution was heated to 65 °C for 6 h and then filtered, and the solvent was removed under vacuum. The residue was extracted with hexane. The hexane extracts were chromatographed on a silica gel plate with hexanes as the eluent. The fastest moving band was collected to give 0.01 g of $Se_2Fe_3(CO)_9$ (0.017 mmol; 5.0% based on Se). The second band was collected to give 0.08 g (0.15 mmol) of $Fe_2(CO)_6(\mu\text{-SeCHPhSe})$ (**3**; 45% based on Se). IR (ν_{CO}, hexanes): 2071 m, 2035 vs, 2000 s cm^{-1}. Mp: 82 °C. ^{1}H NMR (DMSO-d_6, 298 K, ppm): 6.14 (s, 1H), 7.25−7.45 (m, 5H). Anal. Calcd for $Fe_2(CO)_6(\mu\text{-SeCHPhSe})$ (**3**): C, 29.58; H, 1.15. Found: C, 29.58; H, 1.21.

Reaction of $[Et_4N]_2[SeFe_3(CO)_9]$ with CH_2I_2. To a solution of 0.690 g (0.91 mmol) of $[Et_4N]_2[SeFe_3(CO)_9]$ in 40 mL of MeCN in an ice/water bath was added 0.08 mL (0.99 mmol) of CH_2I_2 dropwise. The mixed solution was stirred in the ice/water bath for 3 h and then warmed to 30 °C and stirred for another 48 h. The resultant reddish brown solution was filtered, and the solvent was removed under vacuum. The residue was then extracted with hexanes. The hexane extracts were chromatographed on a silica gel plate with hexanes as the eluent. The fastest moving band was collected to give 0.02 g of $Se_2Fe_2(CO)_6(\mu\text{-}CH_2)_2$ (**4**), which was contaminated with a trace amount of $Se_2Fe_3(CO)_9$. These compounds are difficult to separate by chromatography, and the structure determination of **4** was carried out by X-ray analysis. The second band was collected to give 0.02 g (0.043 mmol) of $Se_2Fe_2(CO)_6(CH_3)_2$ (9% based on Se). IR (ν_{CO}, hexanes): 2064 m, 2033 vs, 1992 vs, br cm^{-1}. ^{1}H NMR ($CDCl_3$, 298 K, ppm): 2.10 (s). ^{13}C NMR ($CDCl_3$, 298 K, ppm): 7.6, 209.9. Mp: 134 °C dec. Mass (EI, 20 eV): M^+, *m/e* 470. The third band gave 0.02 g (0.044 mmol) of $Fe_2(CO)_6(\mu\text{-SeCH}_2\text{Se})$ (9% based on Se). IR (ν_{CO}, hexanes): 2071 m, 2033 vs, 2000 vs, br cm^{-1}. ^{1}H NMR ($CDCl_3$, 298 K, ppm): 4.02 (s). ^{13}C NMR ($CDCl_3$, 298 K, ppm): 27.5, 209.4.

X-ray Structural Characterization of Complexes 1−3. A summary of selected crystallographic data for **1**−**3** is given in Table 1. Data collection was carried out on a Nonius CAD-4 diffractometer using graphite-monochromated Mo Kα radiation at 25 °C. All crystals were mounted on glass fibers with epoxy cement. Data reduction and structural refinement were performed using the NRCC-SDP-VAX packages,[8] and atomic scattering factors were taken from ref 9.

Structures of 1−3. The black crystal of **1** chosen for diffraction measurement had the dimensions ca. 0.10 × 0.13 × 0.55 mm; those for the black crystal of **2** were 0.10 × 0.10 × 0.50 mm and for the red crystal of **3** were 0.25 × 0.50 × 0.50 mm. Cell parameters were obtained from 25 reflections with 2θ angles in the range 14.46−25.32° for **1**, 20.00° < 2θ < 29.52° for **2**, and 19.16° < 2θ < 32.28° for **3**. A total of 3307 reflections with $I > 2.0\sigma(I)$ for **1** (4114 reflections with $I > 2.0\sigma(I)$ for **2** and 2148 reflections with $I > 2.0\sigma(I)$ for **3**) were used in the refinement. The structures were solved by the heavy-atom method and refined by least-squares cycles. All the non-hydrogen atoms were refined with anisotropic temperature factors. Full-matrix least-squares refinement led to convergence with $R = 4.4\%$ and $R_w = 4.1\%$ for **1**, with $R = 3.9\%$ and $R_w = 3.6\%$ for **2**, and with $R = 2.9\%$ and $R_w = 2.8\%$ for **3**.

Since the structure of **4** was reported recently,[7] the details of the X-ray determination for **4** are omitted here. Selected distances and angles for **1**−**3** are given in Tables 2−4, respectively. Additional crystallographic data are available as Supporting Information.

Results

Reactions of $[SeFe_3(CO)_9]^{2-}$ with Electrophiles. The reactions of the *closo*-tetrahedral cluster $[SeFe_3(CO)_9]^{2-}$ with a series of electrophiles were investigated.

(8) Gabe, E. J.; Lepage, Y.; Charland, J. P.; Lee, F. L.; White, P. S. *J. Appl. Crystallogr.* **1989**, *22*, 384.
(9) *International Tables for X-ray Crystallography*; Kynoch Press: Birmingham, England, 1974; Vol. IV.

Table 2. Selected Bond Distances (Å) and Bond Angles (deg) for $[Et_4N]_2[SeFe_2Ru_3(CO)_{14}]$ (1)[a]

(A) Distances

Se−Ru(1)	2.544(2)	Se−RF	2.512(2)
Se−Ru(3)	3.505(1)	Se−FR	2.438(2)
Se−Fe(2)	2.349(2)	Ru(1)−RF	2.784(2)
Ru(1)−Ru(3)	2.822(1)	Ru(1)−FR	2.761(2)
RF−Ru(3)	2.854(1)	RF−Fe(2)	2.745(2)
Ru(3)−FR	2.757(2)	Ru(3)−Fe(2)	2.731(2)
FR−Fe(2)	2.714(2)		

(B) Angles

Ru(1)−Se−RF	66.81(4)	Ru(1)−Se−Ru(3)	52.75(3)
Ru(1)−Se−FR	67.27(5)	Ru(1)−Se−Fe(2)	103.78(6)
RF−Se−Ru(3)	53.59(3)	RF−Se−FR	105.04(6)
RF−Se−Fe(2)	68.67(5)	Ru(3)−Se−FR	51.54(4)
Ru(3)−Se−Fe(2)	51.06(4)	FR−Se−Fe(2)	69.06(6)
Se−Ru(1)−RF	56.04(4)	Se−Ru(1)−Ru(3)	81.39(4)
Se−Ru(1)−FR	54.53(4)	RF−Ru(1)−Ru(3)	61.20(3)
RF−Ru(1)−FR	90.22(4)	Ru(3)−Ru(1)−FR	59.17(4)
Se−FR−Ru(1)	58.21(4)	Se−FR−Ru(3)	84.64(5)
Se−FR−Fe(2)	53.92(5)	Ru(1)−FR−Ru(3)	61.52(4)
Ru(1)−FR−Fe(2)	89.42(5)	Ru(3)−FR−Fe(2)	59.87(5)
Se−RF−Ru(1)	57.15(4)	Se−RF−Ru(3)	81.31(4)
Se−RF−Fe(2)	52.85(5)	Ru(1)−RF−Ru(3)	60.06(4)
Ru(1)−RF−Fe(2)	88.33(5)	Ru(3)−RF−Fe(2)	58.34(4)
Se−Ru(3)−Ru(1)	45.86(3)	Se−Ru(3)−RF	45.10(3)
Se−Ru(3)−FR	43.82(4)	Se−Ru(3)−Fe(2)	42.00(4)
Ru(1)−Ru(3)−RF	58.74(3)	Ru(1)−Ru(3)−FR	59.31(4)
Ru(1)−Ru(3)−Fe(2)	87.84(4)	RF−Ru(3)−FR	88.85(4)
RF−Ru(3)−Fe(2)	58.84(5)	FR−Ru(3)−Fe(2)	59.29(5)
Se−Fe(2)−RF	58.47(5)	Se−Fe(2)−Ru(3)	86.94(6)
Se−Fe(2)−FR	57.02(5)	RF−Fe(2)−Ru(3)	62.82(4)
RF−Fe(2)−FR	92.03(6)	Ru(3)−Fe(2)−FR	60.84(5)

[a] RF = $^3/_4$ Ru + $^1/_4$ Fe; FR = $^3/_4$ Fe + $^1/_4$ Ru.

Table 3. Selected Bond Distances (Å) and Bond Angles (deg) for $[Et_4N][SeFe_3(CO)_9(\mu\text{-HgI})]$ (2)

(A) Distances

Hg(1A)−Fe(1A)	2.605(2)	Hg(1A)−Fe(2A)	2.608(2)
Se(1A)−Fe(1A)	2.314(3)	Se(1A)−Fe(2A)	2.302(2)
Se(1A)−Fe(3A)	2.307(3)	Fe(1A)−Fe(2A)	2.887(3)
Fe(1A)−Fe(3A)	2.624(3)	Fe(2A)−Fe(3A)	2.615(3)
Hg(1A)−I(1A)	2.641(1)		

(B) Angles

I(1A)−Hg(1A)−Fe(1A)	145.33(6)	I(1A)−Hg(1A)−Fe(2A)	145.33(6)
Fe(1A)−Hg(1A)−Fe(2A)	67.26(6)	Fe(1A)−Se(1A)−Fe(2A)	77.45(8)
Fe(1A)−Se(1A)−Fe(3A)	69.18(9)	Fe(2A)−Se(1A)−Fe(3A)	69.12(8)
Hg(1A)−Fe(1A)−Se(1A)	107.51(8)	Hg(1A)−Fe(1A)−Fe(3A)	86.64(8)
Se(1A)−Fe(1A)−Fe(3A)	55.29(8)	Hg(1A)−Fe(2A)−Se(1A)	107.77(8)
Hg(1A)−Fe(2A)−Fe(3A)	86.77(8)	Se(1A)−Fe(2A)−Fe(3A)	55.54(8)
Se(1A)−Fe(3A)−Fe(1A)	55.53(8)	Se(1A)−Fe(3A)−Fe(2A)	55.35(8)
Fe(1A)−Fe(3A)−Fe(2A)	66.91(8)		

Table 4. Selected Bond Distances (Å) and Bond Angles (deg) for $Fe_2(CO)_6(\mu\text{-SeCHPhSe})$ (3)

(A) Distances

Se(1)−Se(2)	2.8747(7)	Se(1)−Fe(1)	2.3762(9)
Se(1)−Fe(2)	2.3894(8)	Se(2)−Fe(1)	2.3882(9)
Se(2)−Fe(2)	2.3795(9)	Fe(1)−Fe(2)	2.5204(9)

(B) Angles

Se(2)−Se(1)−Fe(1)	53.08(2)	Se(2)−Se(1)−Fe(2)	52.77(2)
Fe(1)−Se(1)−Fe(2)	63.86(3)	Se(1)−Se(2)−Fe(1)	52.70(2)
Se(1)−Se(2)−Fe(2)	53.09(2)	Fe(1)−Se(2)−Fe(2)	63.83(3)
Se(1)−Fe(1)−Se(2)	74.22(3)	Se(1)−Fe(1)−Fe(2)	58.33(3)
Se(2)−Fe(1)−Fe(2)	57.92(3)	Se(1)−Fe(2)−Se(2)	74.14(3)
Se(1)−Fe(2)−Fe(1)	57.82(3)	Se(2)−Fe(2)−Fe(1)	58.26(2)

There are basically four types of clusters that result from these reactions. Reaction of $[Et_4N]_2[SeFe_3(CO)_9]$ with $Ru_3(CO)_{12}$ in refluxing acetone formed the heterometallic octahedral cluster $[Et_4N]_2[SeFe_2Ru_3(CO)_{14}]$ (**1**). The IR spectrum of **1** showed terminal carbonyl absorptions in the range 2029−1969 cm^{-1} and a weak peak at 1749 cm^{-1} characteristic of the doubly bridging CO groups. The formulation and structure of **1** were further established by X-ray diffraction analysis.

Further reaction of $[Et_4N]_2[SeFe_3(CO)_9]$ with the mercury electrophile HgI_2 formed a new cluster by sharing one of the Fe−Fe bonds with the incoming species HgI to form the HgI-bridged complex $[Et_4N][SeFe_3(CO)_9HgI]$ (**2**). Cluster **2** has an infrared spectrum identical in pattern with that of $[SeFe_3(CO)_9]^{2-}$, but shifted to higher frequencies, indicative of the dispersion of the electron density of the parent cluster to the HgI moiety.

When $[SeFe_3(CO)_9]^{2-}$ reacted with organic geminal halides such as $PhCHCl_2$, the PhCH bridging butterfly cluster $Fe_2(CO)_6(\mu\text{-SeCHPhSe})$ (**3**) was formed. Obviously, the formation of cluster **3** involved complicated bond breakage and formation processes. The Se···Se distance of 2.8747(7) Å shows no formal Se−Se bond; however, a certain degree of intramolecular interaction is suggested.[10] On the other hand, treatment with CH_2I_2 formed the recently reported $Se_2Fe_2(CO)_6(\mu\text{-}CH_2)_2$ (**4**), $Fe_2(CO)_6(\mu\text{-}SeCH_2Se)$, and $Se_2Fe_2(CO)_6(CH_3)_2$.[7] The last two products are structurally similar to cluster **3**, whereas the cluster **4** displays a different arrangement for the Se_2Fe_2 metal core. Notably, there is no planar Se_2Fe_2 cluster analogous to **4** obtained in the case with $PhCHCl_2$ as the alkylation reagent. It is believed that the failure to form the planar Se_2Fe_2 cluster in the latter case can be attributed to the steric hindrance of the CHPh fragment.

Further reaction of $[SeFe_3(CO)_9]^{2-}$ with $Mn_2(CO)_{10}$ or $[Mn(CO)_3(MeCN)_3]PF_6$[11] in MeCN, however, formed the monohydrido cluster $[HSeFe_3(CO)_9]^-$, and the methylation of $[SeFe_3(CO)_9]^{2-}$ also gave $[HSeFe_3(CO)_9]^-$ as the major product. The tendency to form $[HSeFe_3(CO)_9]^-$ in these cases is probably due to the weak affinity between these electrophiles and $[SeFe_3(CO)_9]^{2-}$. The formation of $[HSeFe_3(CO)_9]^-$ could be due to the reaction of $[SeFe_3(CO)_9]^{2-}$ with moisture in the air or the trace amount of H_2O in the solvent.

The reactions of $[SeFe_3(CO)_9]^{2-}$ with the electrophiles $Ru_3(CO)_{12}$, HgI_2, $PhCHCl_2$, and CH_2I_2 are summarized in Scheme 1.

Crystal Structures of 1−3. Complexes **1**−**3** have been structurally characterized by spectroscopic methods and X-ray diffraction analyses. Cluster **1** displays an octahedral metal core with a μ_4-Se atom and two carbonyl groups bridging the Ru−Ru and Ru−Fe bonds (Figure 1). X-ray analysis shows that it is not possible to distinguish the positions of one iron and one ruthenium atom. However, elemental analysis confirmed the formulation as $[Et_4N]_2[SeFe_2Ru_3(CO)_{14}]$. Complex **2** displays a $SeFe_3$ core with a HgI fragment bridging the Fe−Fe bond (Figure 2). The two crystallographically independent molecules of **2** in the unit cell are only slightly different from each other, and only one of them is discussed here. Cluster **3** exhibits a Se_2Fe_2 butterfly geometry with the two Se wingtips linked by a CHPh moiety (Figure 3).

For comparison, average Se−Fe and Fe−Fe bond distances are listed in Table 5. The average distances of Se−Fe in compounds **1**−**4** are 2.349, 2.308, 2.383, and 2.421 Å, respectively. These values in clusters **1**−**3** are compared to those of the related clusters $[PPN]_2[SeFe_3$-

(10) (a) McConnachie, J. M.; Ibers, J. A. *Inorg. Chem.* **1991**, *30*, 1770. (b) Wolmershäuer, G.; Heckmann, G. *Angew. Chem., Int. Ed. Engl.* **1992**, *31*, 779. (c) Kanatzidis, M. G. *Comments Inorg. Chem.* **1990**, *10*, 161.

(11) Drew, D.; Darensbourg, D. J.; Darensbourg, M. Y. *Inorg. Chem.* **1975**, *14*, 1579.

Scheme 1

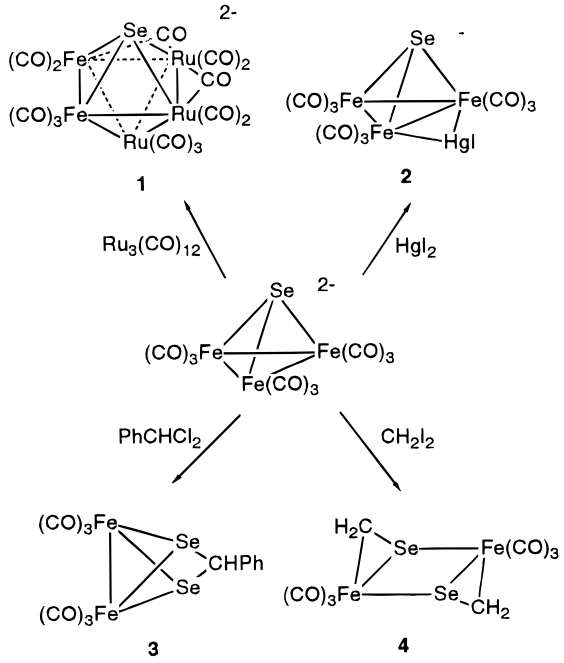

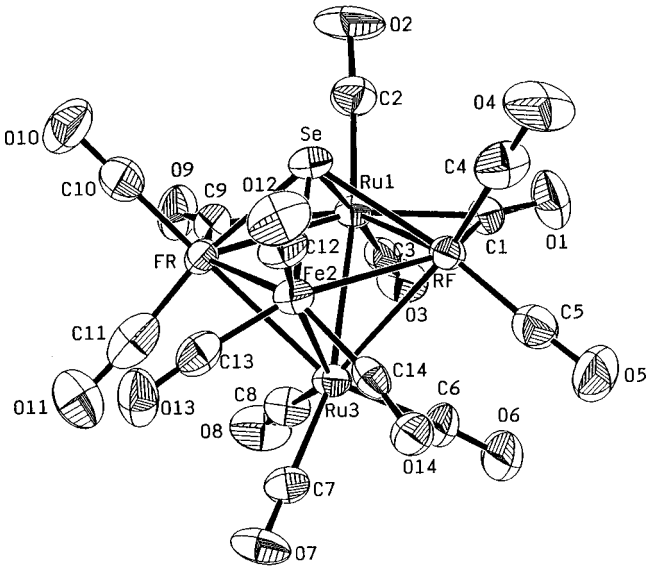

Figure 1. ORTEP diagram showing the structure and atom labeling for the anion of **1** (where RF = $^3/_4$ Ru + $^1/_4$ Fe and FR = $^3/_4$ Fe + $^1/_4$ Ru).

$(CO)_9]$ (2.322 Å)[2b] and $[Et_4N]_2[\{SeFe_3(CO)_9\}_2Hg]$ (2.311 Å).[2a] The longer Se−Fe distance in **4** is due to the presence of the bridging CH_2 group, and the same situation is also observed for the Fe(1A)−Fe(2A) bond of **2** (2.887(3) Å), due to the effect of the bridging HgI fragment.

Discussion

Structures and Bonding in Clusters 1−4. The metal core of cluster **1** displays an octahedral geometry with a μ_4-Se atom bonded to two Fe atoms and two Ru atoms, which is structurally similar to the previously reported cluster $[OFe_2Ru_3(CO)_{14}]^{2-}$.[12] The μ_4-Se atom acts as a four-electron donor to contribute to the metal core, which is consistent with Wade's rule for a six-vertex *closo* cluster containing seven skeletal bonding pairs. Although the μ_4-S bonding mode has been exploited widely,[13] there are relatively fewer studies involving face-capping μ_4-Se metal carbonyl complexes. The structurally characterized examples include $Fe_4(CO)_{10}(\mu\text{-CO})(\mu_4\text{-Se})_2$,[14] $Fe_3Ru(CO)_{10}(\mu\text{-CO})(\mu_4\text{-Se})_2$,[14] and $Ru_4(CO)_{11}(\mu_4\text{-Se})_2$.[15] The distance of Se−Ru(1) is 2.544(2) Å, close to the value 2.584 Å in $Ru_4(CO)_{11}(\mu_4\text{-Se})_2$, and the unbridged Ru(1)−Ru(3) length is 2.822(1) Å, similar to the Ru−Ru bond length of 2.854(4) Å in $Ru_3(CO)_{12}$.[16]

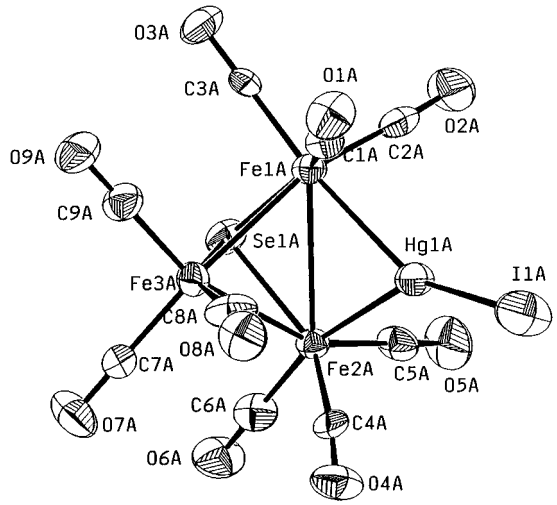

Figure 2. ORTEP diagram showing the structure and atom labeling for the anion of **2**.

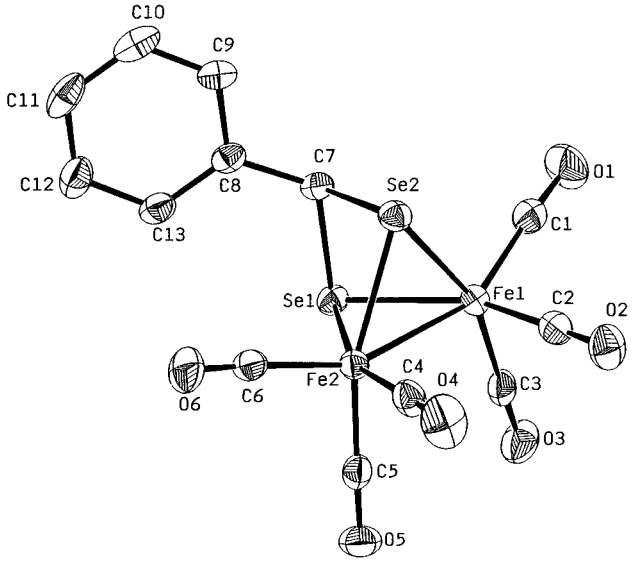

Figure 3. ORTEP diagram showing the structure and atom labeling for **3**.

Table 5. Average Se−Fe and Fe−Fe Distances (Å) of Clusters 1−4 and Other Related Clusters

compd	Se−Fe	Fe−Fe
$[PPN]_2[SeFe_3(CO)_9]$[2b]	2.322	2.610
$[Et_4N]_2[\{SeFe_3(CO)_9\}_2Hg]$[2a]	2.311	2.721
$[Et_4N]_2[SeFe_2Ru_3(CO)_{14}]$ (**1**)[a]	2.349	
$[Et_4N][SeFe_3(CO)_9(\mu\text{-HgI})]$ (**2**)[a]	2.308	2.620
$Fe_2(CO)_6(\mu\text{-SeCHPhSe})$ (**3**)[a]	2.383	2.520
$Se_2Fe_2(CO)_6(\mu\text{-CH}_2)_2$ (**4**)[a]	2.421	

[a] This work.

(12) Schauer, C. K.; Voss, E. J.; Sabat, M.; Shriver, D. F. *J. Am. Chem. Soc.* **1989**, *111*, 7662.

(13) (a) Adams, R. D.; Babin, J. E.; Wang, J. G. *Polyhedron* **1989**, *8*, 2351. (b) Adams, R. D. *Polyhedron* **1985**, *4*, 2003.

(14) Datta, S. N.; Kondru, R.-K.; Mathur, P. *J. Organomet. Chem.* **1994**, *470*, 169.

(15) Johnson, B. F. G.; Layer, T. M.; Lewis, J.; Martín, A.; Raithby, P. R. *J. Organomet. Chem.* **1992**, *429*, C41.

The metal core of **2** can be viewed as the monohydrido cluster $[HSeFe_3(CO)_9]^-$ in which the H atom is replaced by a HgI moiety. HgI^+ functions as H^+ to add to the parent cluster $[SeFe_3(CO)_9]^{2-}$. A HgX fragment occupying an edge-bridging position was first reported in the clusters $[Ru_3(\mu_3\text{-}C_2t\text{Bu})(CO)_9(HgX)]$ (X = Br, I),[17] and cluster **2** represents a new HgI-bridged Se−Fe carbonyl cluster. Cluster **2** can be compared to the isostructural Te−Fe cluster $[TeFe_3(CO)_9CuCl]^{2-}$,[18] in which an intact CuCl fragment bridges one Fe−Fe bond of a $[TeFe_3(CO)_9]^{2-}$ cluster. As also seen in $[TeFe_3(CO)_9CuCl]^{2-}$, the Fe−Fe bond to which the Hg is bound is the longest at 2.887(3) Å, compared with 2.624(3) and 2.615(3) Å for the Fe−Fe bonds which are not bridged by mercury. The Hg−I bond length in **2** is normal at 2.641(1) Å. The HgX-bridged clusters themselves may be employed as Hg fragments in further cluster-building reactions. The incorporation of other metal clusters into **2** is now being attempted.

Cluster **3** displays a butterfly geometry with the wingtips linked by a CHPh fragment. This type of structure is common in chalcogen-containing iron carbonyl clusters such as $Fe_2(CO)_6(\mu\text{-}TeCH_2Te)$,[19] $Fe_2(CO)_6(\mu\text{-}TeCHPhTe)$,[20] $Fe_2(CO)_6(\mu\text{-}SCH_2S)$,[21] $Fe_2(CO)_6(\mu\text{-}SeCH_2Se)$,[7] and $Fe_2(CO)_6(\mu\text{-}SeCH_2Te)$,[22] and cluster **3** provides another addition to this family. The Se−CHPh−Se angle of 93.1(2)° in **3** is larger than the value 92.5(1)° for the Te−CHPh−Te angle of its analog $Fe_2(CO)_6(\mu\text{-}TeCHPhTe)$, which can be compared to the corresponding angle of 92.1(4)° in $Fe_2(CO)_6(\mu\text{-}TeCH_2Te)$, and all these angles are smaller than that (94.2°) reported for $Fe_2(CO)_6(\mu\text{-}SeCH_2Se)$ and that (94.6°) for $Fe_2(CO)_6(\mu\text{-}SCH_2S)$, presumably due to the effect of the size of the chalcogen atoms.

The metal core of cluster **4** contains a Se_2Fe_2 cyclic ring in which two Se−Fe bonds are bridged by two CH_2 groups. The bridged Se−Fe bonds in **4** average 2.401 Å, which is slightly shorter than the value 2.441 Å, found for the unbridged Se−Fe bonds. The average Se−C−Fe angle of 73.7° is smaller than the corresponding angle (76.6°) for $Te_2Fe_2(CO)_6(\mu\text{-}CH_2)_2$.[23] This observation can also be explained by the effect of the different sizes of Se and Te atoms.

Formation of Four Types of Clusters. It is found that the reaction with HgI_2 forms the μ_2-Hg cluster **2**, which differs from the μ_4-Hg cluster $[\{SeFe_3(CO)_9\}_2Hg]^{2-}$ resulting from treatment with $Hg(OAc)_2$. This indicates that the employment of different mercury salts may give rise to clusters with some different structural features. The ease of formation of the μ_2-Hg cluster in the HgI_2 case may be ascribed to the stronger Hg−I bond because of the better soft−soft interaction.

We were curious whether a similar type of heterometallic clusters could be obtained when transition-metal complexes were employed. When the triruthenium cluster $Ru_3(CO)_{12}$ was refluxed with $[SeFe_3(CO)_9]^{2-}$ in acetone, the hexanuclear cluster **1** was obtained. It is assumed that $Ru_3(CO)_{12}$ can eliminate CO in refluxing acetone to form the electrophile $Ru_3(CO)_{10}(Me_2CO)_2$, which may subsequently incorporate $[SeFe_3(CO)_9]^{2-}$ followed by the loss of $Fe(CO)_3$ and CO groups. To accommodate such a large Ru_3 electrophile, the reactive "$SeFe_2$" species, not just the Fe−Fe bond, may be involved in the process of formation of **1**. We wondered whether the reaction with the triiron carbonyl complex $Fe_3(CO)_{12}$ can also give a similar hexanuclear cluster. An independent reaction was conducted; however, there was no such product observed. The stronger metal−metal interaction in $Ru_3(CO)_{12}$, compared to that in $Fe_3(CO)_{12}$, may account for this difference.

It was initially thought that $[SeFe_3(CO)_9]^{2-}$ could react with geminal halides to form tetrahedral clusters with the formula $SeFe_3(CO)_9(\mu\text{-}CR_2)$, which has one Fe−Fe bond or Se−Fe bond bridged by the incoming organo group. Upon alkylation with $PhCHCl_2$, the butterfly Se_2Fe_2 cluster was produced instead. We believe that the steric hindrance of the CHPh moiety prevents the formation of the proposed cluster, and cluster **3** may result from $Fe(CO)_3$ vertex loss and recombination of the resultant species "SeFe" and the organo fragment PhCH. As seen in other chalcogen-containing cluster formations,[24] the Se···Se interaction may play an important role in the formation of cluster **3**.

When the smaller CH_2 group was introduced, the CH_2-bridged cluster $SeFe_3(CO)_9(\mu\text{-}CH_2)$ was still not formed. The failure to form such a species may be attributed to the large bridging group CH_2, as compared to the H bridging atom in the cases of $[HSeFe_3(CO)_9]^-$ and $H_2SeFe_3(CO)_9$. However, the role of the negative charge distribution of $[SeFe_3(CO)_9]^{2-}$ cannot be excluded. In this case, the Se−Fe bridged cluster **4** was obtained along with the Se···Se bridged butterfly cluster $Fe_2(CO)_6(\mu\text{-}SeCH_2Se)$. Together with the outcomes in the $PhCHCl_2$ case, we believe that the size of the CR_2 groups is crucial in the formation of cluster **4**.

In this study, it has been demonstrated that the size, the softness, and the nature of the electrophiles can affect the outcomes of the reactions of the tetrahedral cluster $[SeFe_3(CO)_9]^{2-}$ with incoming electrophiles. Not only the Fe−Fe bonds but also the entire $[SeFe_3(CO)_9]^{2-}$ group, depending on the electrophiles, should be taken into consideration in these reactions.

Acknowledgment. We thank the National Science Council of the Republic of China for financial support (Grant No. NSC 85-2113-M-003-003).

Supporting Information Available: Tables giving all crystallographic data, atomic positional parameters, bond distances and angles, and anisotropic thermal parameters for complexes **1**−**3** (18 pages). Ordering information is given on any current masthead page.

OM960767T

(16) Churchill, M. R.; Hollander, F. J.; Hutchinson, J. P. *Inorg. Chem.* **1977**, *16*, 2655.
(17) Fahmy, R.; King, K.; Rosenberg, E.; Tiripicchio, A.; Tiripicchio-Camellini, M. *J. Am. Chem. Soc.* **1980**, *102*, 3626.
(18) Bachman, R. E.; Whitmire, K. H.; van Hal, J. *Organometallics* **1995**, *14*, 1792.
(19) (a) Mathur, P.; Reddy, V. D. *J. Organomet. Chem.* **1990**, *387*, 193. (b) Mathur, P.; Reddy, V. D. *J. Organomet. Chem.* **1991**, *401*, 339.
(20) Shieh, M.; Chen, P.-F.; Tsai, Y.-C.; Shieh, M.-H.; Peng, S.-M.; Lee, G.-H. *Inorg. Chem.* **1995**, *34*, 2251.
(21) Shaver, A.; Fitzpatrick, P. J.; Steliou, K.; Butler, I. S. *J. Am. Chem. Soc.* **1979**, *101*, 1313.
(22) Mathur, P.; Manimaran, B.; Hossain, M. M.; Shanbag, R.; Murthy, J.; Saranathan, I. S.; Satyanarayana, C. V. V.; Bhadbhade, M. M. *J. Organomet. Chem.* **1995**, *490*, 173.
(23) Mathur, P.; Manimaran, B.; Hossain, M. M.; Satyanarayana, C. V. V.; Puranik, V. G.; Tavale, S. S. *J. Organomet. Chem.* **1995**, *493*, 251.
(24) Shieh, M.; Tang, T.-F.; Peng, S.-M.; Lee, G.-H. *Inorg. Chem.* **1995**, *34*, 2797.